

Dried leaf *Artemisia annua* efficacy against non-small cell lung cancer

Dina J. Rassias^a, Pamela J. Weathers^{b,*}

^a Department of Biomedical Engineering, Worcester Polytechnic Institute, United States

^b Department of Biology and Biotechnology, Worcester Polytechnic Institute, Worcester, MA 01609 United States

ARTICLE INFO

Keywords:

Artemisinin
Artesunate

ABSTRACT

Background: Non-small cell lung cancer (NSCLC) is a major subtype of lung cancer with poor prognosis. Artemisinin (AN), produced naturally in *Artemisia annua* L., has anti-cancer activity. Artemisinin delivered as dried leaf *Artemisia* (DLA) showed efficacy against malaria in rodents and humans.

Hypothesis/Purpose: DLA is posited as being at least as efficacious as artesunate (AS) in its ability to induce cytotoxicity in NSCLC cells and also inhibit tumor growth in a NSCLC xenograft murine model.

Study Design: Three NSCLC cell lines were used, a non-cancerous human fibroblast line, and xenograft murine models to compare efficacy of artemisinin delivered *p.o.* via DLA, DLA extracts (DLAe), and AS.

Methods: DLAe was compared to AS using NSCLC cell lines A549, H1299 and PC9 as well as non-cancerous human dermal fibroblasts (HDF) CCD-1108Sk line. Cell viability, cell migration and cell cycle were compared for AS and DLAe. Westerns measured activated caspases-3, -8 and -9 to determine involvement of intrinsic and/or extrinsic apoptotic pathways. Xenograft murine models of A549 and PC9 cells were used to measure tumor growth inhibition by AS or DLA, with tumor volume the primary endpoint.

Results: Both DLAe and AS suppressed A549, H1299 and PC9 cell viability with no inhibition of non-cancerous HDF CCD-1108Sk cells. Caspases-3, -8 and -9 were activated, suggesting cell death was stimulated through both intrinsic and/or extrinsic apoptotic pathways. Both drugs induced G2/M or mitotic arrest in PC9 and H1299 cells, and DLAe induced G1 arrest in A549 cells. AS and DLAe induced DNA damage as double stranded breaks evidenced by phosphorylation of histone H2AX. DLAe inhibited migration of PC9 and A549 cells. In A549 xenografted animals, *p.o.* AS and DLA inhibited relative tumor growth by 40% and 50%, respectively, compared to controls. AS was ineffective at inhibiting PC9-induced tumor growth, but DLA inhibited relative tumor growth by ~50% compared to controls.

Conclusion: This is the first study demonstrating efficacy of DLA and mechanistic differences of DLAe vs. AS, against NSCLC cells. Compared to AS, DLA possesses qualities of a novel therapeutic for patients with NSCLC.

Introduction

Non-small cell lung cancer (NSCLC) accounts for ~80% of lung cancers and has poor prognosis (Saito et al., 2017). Semi-synthetic derivatives of artemisinin (AN; Fig. 1A), a sesquiterpene lactone produced in *Artemisia annua* L., demonstrated anti-cancer activity (Lai et al., 2013; Efferth, 2017). *A. annua* is generally recognized as safe (GRAS) (Duke, 1992). Mechanisms for anti-cancer activity of AN rely mainly on generation of reactive oxygen species (ROS) resulting from interaction of the endoperoxide bridge with either free ferrous iron or haem iron (O'Neill and Posner, 2004; Wang et al., 2015). Increased

requirements for iron in cancer cells and higher intake of iron through transferrin receptors, typically overexpressed on cancer cells, makes them more susceptible to damage by ROS from an iron catalyzed reaction with AN (Kwok and Richardson, 2002; Efferth et al., 2004; Lai and Singh, 1995). The reaction likely occurs in cancer cells with increased iron (Lai et al., 2013) and enhanced haem biosynthesis compared to healthy cells (Hooda et al., 2013), making artemisinins a safer and attractive alternative to current chemotherapies.

AS, AM, and DHA are AN semi-synthetic derivatives all containing the endoperoxide bridge, functioning mechanistically the same (Lee and Hufford, 1990) (Fig. 1B), are currently approved malaria

Abbreviations: AM, artemether; AN, artemisinin; AS, artesunate; DHA, dihydroartemisinin; DLA, dried leaf *Artemisia*; DLAe, dried leaf *Artemisia* extract; GRAS, generally recognized as safe; HDF, human dermal fibroblast; IACUC, institutional animal care and use committee; NSCLC, non-small cell lung cancer; MeCl₂, methylene chloride; MTT, 3-(4,5-Dimethyl-2-thiazolyl)-2,5-diphenyl-2H-tetrazolium bromide; PBS, phosphate buffered saline; *p.o.*, per os; ROS, reactive oxygen species; SEM, standard error of the mean; WHO, World Health Organization

* Corresponding author.

E-mail address: weathers@wpi.edu (P.J. Weathers).

<https://doi.org/10.1016/j.phymed.2018.09.167>

Received 4 September 2018; Accepted 17 September 2018

0944-7113/© 2018 Elsevier GmbH. All rights reserved.

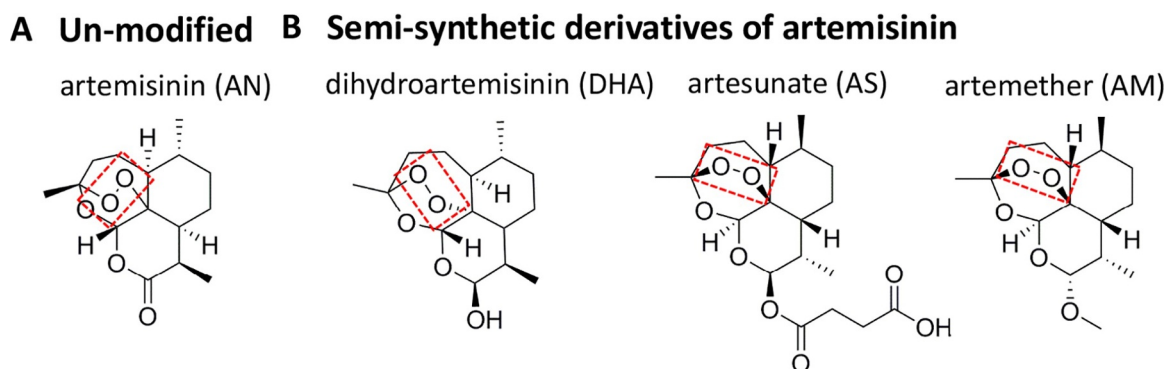


Fig. 1. (A) Artemisinin and (B) its derivatives.

Table 1.

IC₅₀ values for AS and AN in DLAE.

Cell line	AS (μM)	DLAe (μM)
PC9 24 h	142.89	56.31
48 h	51.04	37.20
H1299 24 h	60.75	77.49
48 h	9.19	47.43
A549 24 h	104.13	169.77
48 h	35.34	74.82

therapeutics (WHO, 2015), and therefore are available for treating other ailments including neoplasms.

AS is one of the more studied AN derivatives with cytotoxic action against many cancers (Efferth et al., 2003). A less costly alternative is dried *A. annua* leaves (DLA) (Elfawal et al., 2012; Weathers et al., 2014). DLA may be equally, if not more effective, than semi-synthetic AN derivatives against cancer because the plant contains other anticancer phytochemicals including flavonoids, coumarins, and essential oils (Ferreira et al., 2010; Efferth et al., 2011).

AN derivatives, AS, DHA and AM, slow proliferation, induce cell cycle arrest, induce apoptosis, prevent migration and invasion, inhibit angiogenesis in NSCLC cell lines, and slow tumor growth in NSCLC xenograft models (Table S1). Here we compare DLA extracts (DLAe) with AS in three NSCLC cell lines and DLA with AS in two murine xenograft models.

Materials and methods

Plant material and extraction

Artemisia annua L. clonal SAM cultivar (voucher MASS 317,314) producing approximately 1.1% AN w/w was used; phytochemical contents are detailed in Weathers and Towler (2014). Methylene chloride (MeCl₂) extracts of AN are more cytotoxic to cancer cells than methanol extracts (Efferth et al., 2011), so MeCl₂ was the chosen solvent. Extracts of AN were used for *in vitro* studies, however powdered whole plant DLA was used for *in vivo* studies and sieved through a 0.2 mm mesh for *per os* (*p.o.*) delivery. Quantification of AN in DLA using gas chromatography-mass spectrometry (GC-MS) is detailed in (Weathers and Towler, 2014).

Cell lines

Human NSCLC cell line A549 was purchased from ATCC (CCL-185); PC9 cells were from Amity Manning (WPI); H1299 and human dermal fibroblast (HDF), CCD-1108Sk cells were from Tanja Dominko (WPI). Gifted lines were validated by Genetica DNA Laboratories LabCorp (Supplemental material).

Cell maintenance and drug treatment

NSCLC cells were maintained in RPMI-1640 media supplemented with L-glutamine (Genesee Scientific) and 10% fetal bovine serum at 5% CO₂, 37 °C and atmospheric oxygen. HDFs were cultured in DMEM/F12 media supplemented with 4 mM L-glutamine (Corning) and 10% fetal clone III (Hyclone) at 5% CO₂, 37 °C and atmospheric oxygen. AS (Pharmahonoi Batch PHA-160,802), DLAe and AS were dissolved in DMSO at stock concentrations of 100 mM of AN or AS and stored at – 20 °C. Either AS, DLAe, or DMSO was added to the media for *in vitro* studies. DMSO was always ≤ 0.2%.

Viability

Viability was measured using MTT assay (#M5655, Sigma). Cell densities of 4 × 10³ (24 h) or 2.5 × 10³ (48 h) cells per 100 μl were seeded into each well in a 96-well plate, settled overnight, and then, AS or equal molar amounts of AN in DLAe were diluted in 50 μl of medium, added to each well at 0–200 μM and incubated for 24 or 48 h at 37 °C. After incubation, a 5 mg/ml MTT stock solution in phosphate buffered saline (PBS) was added to each well at 10% well volume, and incubated at 37 °C for 3.25 h. Medium was then replaced with 100 μl DMSO, shaken 10 min at room temperature and absorbance (570 nm) measured with six technical replicates per condition. A standard curve correlated absorbance with cell number. Results were normalized to DMSO controls representing 100% viability. Mean concentrations were interpolated using Microsoft Excel ED50plus v1.0 plugin to estimate the concentration correlating to 50% viability (IC₅₀).

Cell cycle

A549, PC9 or H1299 were seeded at 5 × 10⁵ cells in 60 mm tissue culture plates, settled overnight, then treated with either AS or DLAe based on estimated IC₅₀ values vs. DMSO-treated control cells. Adherent cells were harvested, fixed 24 h post treatment, rinsed with PBS, trypsinized, re-suspended in 300 μl of PBS and added drop wise to 700 μl of iced 100% ethanol. After two PBS rinses, cells were digested with 50 μl of 100 μg/ml RNase A (Amresco), and incubated with 200 μl of 50 μg/ml propidium iodide (Thermo Fisher Scientific) for 30 min at room temperature. Using a BD Accuri C6 Flow Cytometer, 40,000 events were collected and analyzed.

Migration

A wound-healing assay measured drug inhibition of cell migration. Mitomycin C, 1% serum in media and sub-IC₅₀ drug concentrations were used to exclude proliferation or apoptosis as potential confounding variables in measuring cell migration. Cells were seeded at 5 × 10⁵ per well in 6-well tissue culture plates. At confluency, 10 μg/ml of mitomycin C (Calbiochem #475,820) was added for 2 h, then the

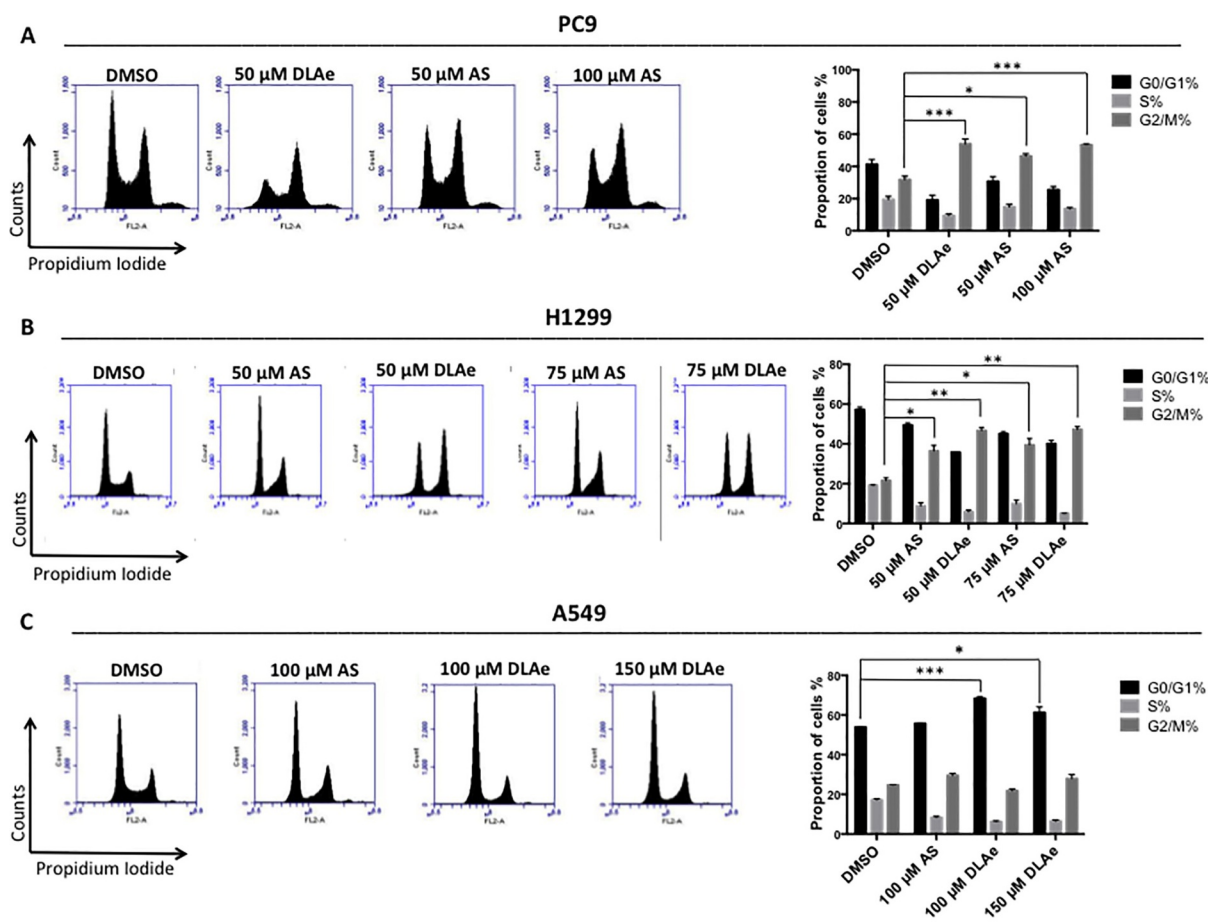


Fig. 2. Effects of AS and DLAE on cell cycle progression in NSCLC cell lines. Cell cycle histograms and percentage of (A) PC9, (B) H1299, and (C) A549 cells in G0/G1, S, and G2/M phases after 24 h treatment with DMSO, AS or DLAE as detected by flow cytometry. ($n = 3$; 2 for PC9 50 μM AS; $* p < 0.05$, $** p < 0.01$, $*** p < 0.001$ compared to DMSO).

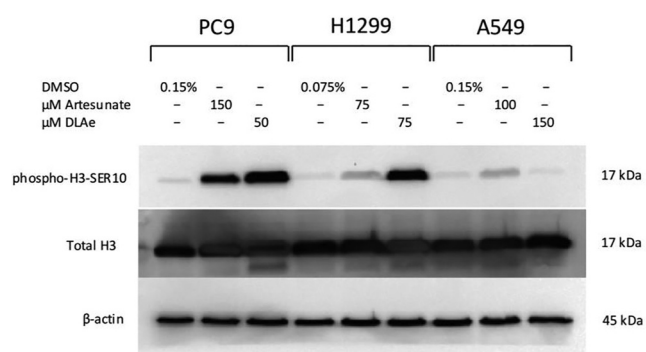


Fig. 3. Artesunate (AS) and DLAE arrest PC9 and H1299 cells in mitosis. Protein from whole cell lysates of NSCLC PC9, H1299, and A549 cells after 24 h treatment with DMSO, artesunate (AS), or DLAE examined by Western blot with phospho-H3-Ser10 antibodies. β -actin was loading control; total histone H3 was nuclear loading control. Representative image from 3 independent experiments.

adherent monolayer was scratched using a P-200 pipette tip and cellular debris gently removed by rinsing twice with PBS. Cells were then treated with DMSO or sub- IC_{50} AS or DLAE in media with 1% FBS. Phase contrast images of fixed positions in the monolayers were taken immediately after initiation of the scratch and again 24 h post treatment. ImageJ was used to quantify cells that migrated into the wound.

Western blotting

Western blotting measured caspases-3, -8, and -9 and phosphorylation of H2A.X and H3-Ser10. Cells treated with either AS or DLAE based on IC_{50} values or DMSO as controls, including those in the supernatant, were harvested 24 h post treatment. Cells were lysed in 2X Laemmli buffer (Bio-Rad #1,610,737) with 5% β -mercaptoethanol (Sigma) at a density of 10^7 cells/ml, boiled 5 min and stored at -20°C . Protein at 20 μl per well was resolved by SDS-PAGE electrophoresis on a 12% or 15% gel and transferred onto a polyvinylidene difluoride membrane (Biorad #162-0177), blocked in 5% non-fat milk or 5% BSA in TBST: 1X TBS containing 0.1% Tween-20 (Boston BioProducts), for 1 h at room temperature and then incubated with primary antibodies: anti-cleaved caspase-8 #9496, anti-cleaved caspase-3 #9664, anti-cleaved caspase-9 #9501, anti-phospho-Histone H3 (Ser10) #9706, anti-phospho-Histone H2A.X #2577, anti- α -tubulin #12,351, anti- β -actin #12,262 (Cell Signaling Technologies), or total histone H3 #1791 (Abcam) diluted in the same blocking solution at 1:1000 dilution overnight at 4°C . The membrane was washed three times, 5 min each, in TBST and with exception of pre-conjugated antibodies α -tubulin or β -actin, subsequently incubated with horseradish peroxidase (HRP)-conjugated goat anti-mouse or goat anti-rabbit secondary antibody (Biorad #170-6515 and #170-6515, respectively) in 1% milk or BSA in TBST at 1:5000 dilution for 1 h at room temperature. After three, 5 min washes in TBST, the membrane was enhanced using a chemiluminescence SuperSignal West Dura Extended Duration Substrate detection kit (Thermo Scientific) and exposed using a Bio-Rad ChemiDoc station and Quantity One software. Images having weak signals were transformed

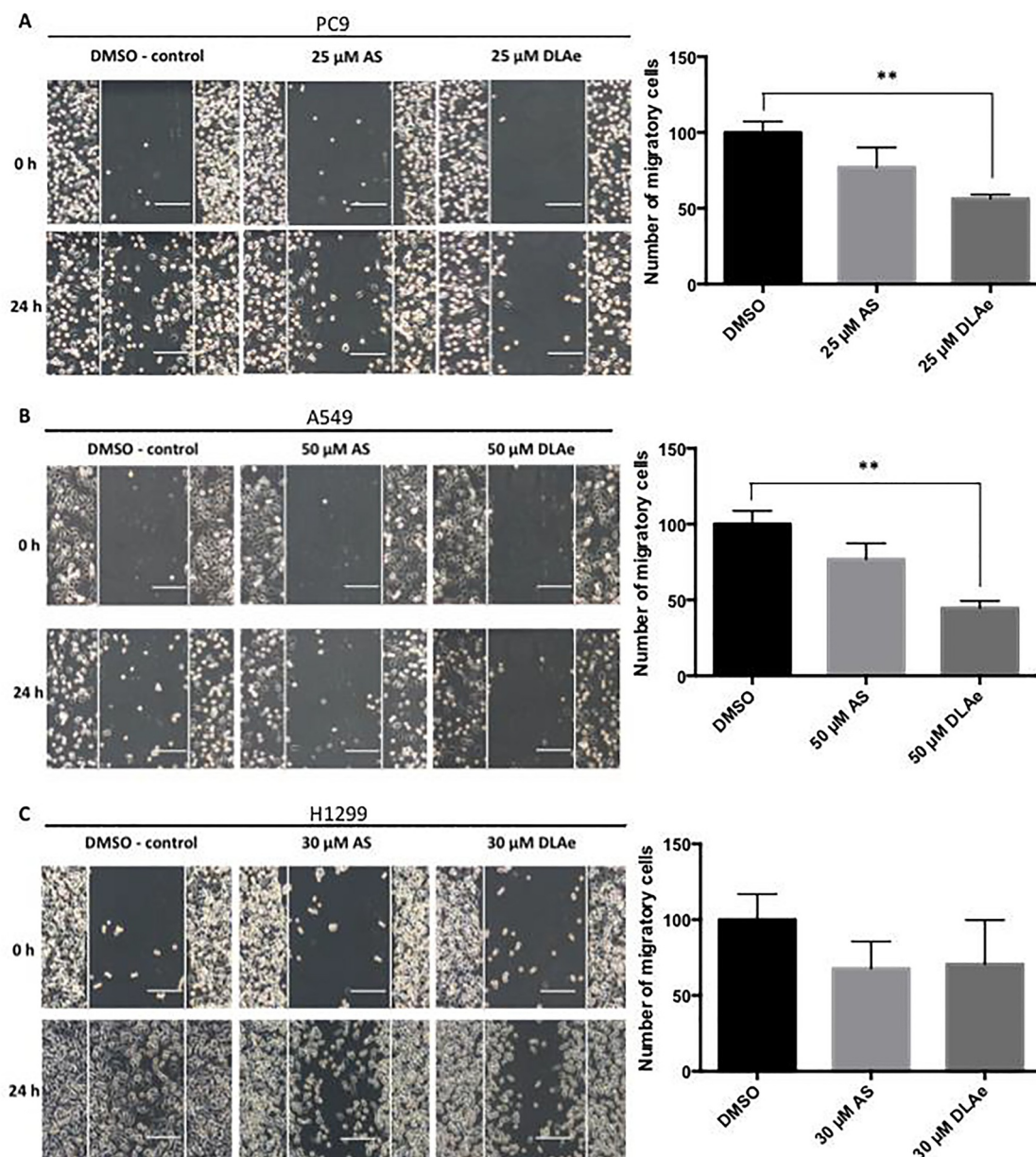


Fig. 4. Migratory effect of AS vs. DLAE in A549 cells. Representative images and summarized migration ratios in wound healing assay: (A) PC9, (B) A549, and (C) H1299 cells from 3 independent experiments (** $p < 0.01$). Scale = 200 μ m.

by adjusting contrast for better visualization; transformation does not alter relative data.

Xenografts

Animal experiments were performed after approval and in accordance with the WPI Institutional Animal Care and Use Committee (IACUC) protocol #15–72. Six-week old female nu/nu mice (Charles River Laboratories - Wilmington - RMS) were used. NSCLC cells were grown, harvested, rinsed with PBS, re-suspended to 5×10^6 (PC9) or 4×10^6 (A549) cells in 200 μ l PBS and injected subcutaneously into the right posterior flank region using a 26 G needle. When palpable tumor masses were about 100 mm^3 , animals were randomized into three groups ($n = 4$ animals per group) and administered *p.o.* gavage daily for 14 days with either AS in water, powdered DLA in water, or water as control. AS or DLA was prepared at the equivalent molar amount of 85 mg AN/kg body weight. Control animals were gavaged the equivalent water volume. Food was withheld 6 h before gavage after which

food access was *ad libitum*. Immediately after preparation, each drug or control treatment was administered daily *p.o.* using a 20 G feeding needle for two weeks. Every 2 days tumor size was measured with calipers and volume calculated as $V = (L \times W^2)/2$. After two weeks, or if tumors reached maximum size of 1.5 cm in either direction, animals were euthanized and tumors excised.

Statistical data analysis

Results were expressed as mean \pm SEM of ≥ 3 biological replicates, unless otherwise stated. *In vitro* data were analyzed using one-way ANOVA with Tukey's post hoc test and *in vivo* data were analyzed using both repeated-measures one-way ANOVA (for differences in tumor volume on day 14) and one-way ANOVA (for differences in relative change in tumor volume) with Tukey's post hoc test using GraphPad Prism software. Differences were significant for $p < 0.05$.

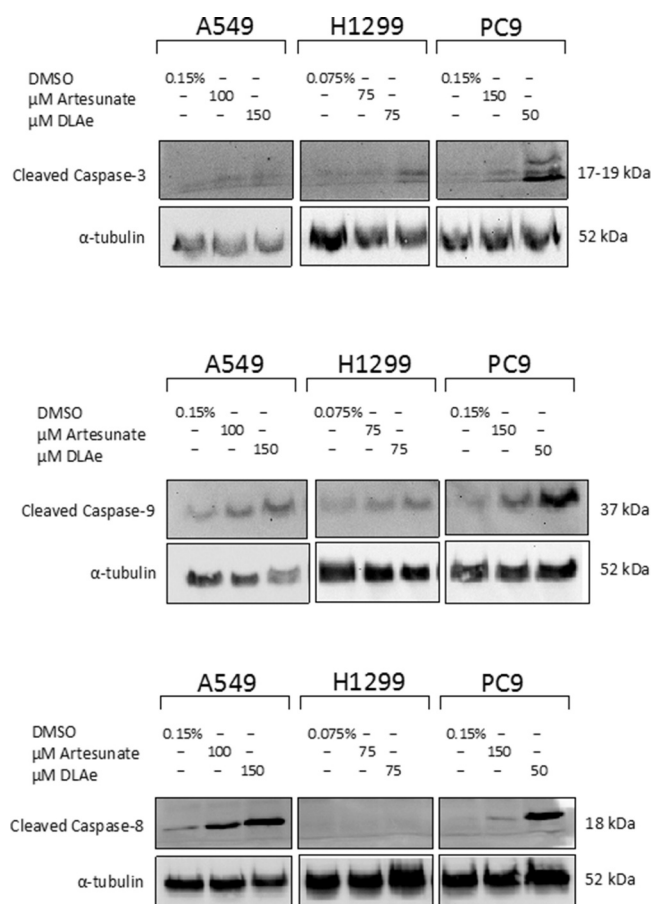


Fig. 5. Apoptosis induction by AS and DLAE. Protein from whole cell lysates of NSCLC PC9, H1299, and A549 cells after 24 h treatment with either DMSO, artesunate (AS), or DLAE were examined by Western blotting with antibodies for cleaved versions of caspase – 3, – 9, or – 8; α -tubulin was loading control. Representative images from 3 independent experiments.

Results

Cytotoxic effects of AS or DLAE on NSCLC cell lines

NSCLC cells treated with AS or DLAE for 24 h exhibited morphological changes associated with apoptosis (Fig. S1). MTT assay showed a dose-dependent inhibition of proliferation in all three cell lines when exposed to AS or DLAE (0–200 μ M) for 24 or 48 h (Fig. S1B). IC_{50} values were in the micromolar range for both drugs and all were lower at 48 h than at 24 h (Table 1). There was no significant solvent effect on viability from either DMSO or MeCl₂ compared to controls (Fig. S2).

There was no effect on viability of non-cancerous HDFs treated with AS and DLAE concentrations \leq 100 μ M compared to DMSO-treated controls. At 150 or 200 μ M for 24 h, percent viability declined < 10% relative to DMSO controls (Fig. S3A). Interestingly, viability increased in HDFs after 24 h treatment with \geq 18.75 μ M DLAE (Fig. S3B).

Phosphorylation of histone H2AX protein increased in all three NSCLC cell lines treated with either AS or DLAE for 24 h indicating cell death may be occurring by overcoming the threshold of repairable DNA damage (Fig. S4).

AS- and DLAE-induced cell cycle arrest in NSCLC cells

Treatment with AS or DLAE for 24 h in PC9 and H1299 increased cells in G2/M phase. PC9 cells after 24 h treatment with 50 μ M AS or DLAE increased significantly, 46.4% or 54.0%, respectively, compared to controls with 31.8% in G2/M phase (Fig. 2A). AS at 100 μ M, a

concentration close to its IC_{50} value, for 24 h also increased cells in the G2/M phase to 53.3%. H1299 cells in the G2/M phase after 24 h exposure to 50 μ M AS or DLAE, were 36.5% and 46.7%, respectively, or when increased to 75 μ M AS or 75 μ M DLAE, were 39.5% and 47.2%, respectively, compared to controls at 21.5% (Fig. 2B). Cell cycle responses were different, however, for A549 cells. After 24 h treatment with 100 or 150 μ M DLAE, cells in G1 phase increased to 61.3% or 68.4%, respectively, compared to controls at 53.9% (Fig. 2C). G1 cell populations treated with 150 μ M AS at 56.2% did not differ compared to controls. These results showed both drugs induced G2/M cell cycle arrest in PC9 and H1299 cells and DLAE induced G1 cell cycle arrest in A549 cells. To corroborate the G2/M arrest, phosphorylation status of histone H3 at Ser10 in Western blots showed increased phospho-H3-Ser10 protein in AS- and DLAE-treated PC9 and H1299 cells (Fig. 3).

AS and DLAE inhibit migratory ability of NSCLC cells

The wound-healing assay showed that after 24 h, DLAE reduced the number of migratory PC9 or A549 cells into the wound by almost 50% (Fig. 4A,B), but did not inhibit migration of H1299 cells (Fig. 4C).

AS and DLAE induced caspase – 3, – 8, and – 9 activation in NSCLC cells

Cleaved caspases – 3, – 8, and – 9 were analyzed for intrinsic and/or extrinsic apoptotic pathway involvement. Treatment with AS or DLAE near their IC_{50} s for 24 h, increased protein levels of cleaved caspase-9 and caspase-3 in all cells compared to controls (Fig. 5). Cleaved caspase-8 levels also increased in A549 and PC9 cells, but not in H1299 cells (Fig. 5).

DLA suppresses tumor growth in NSCLC murine xenografts

After *p.o.* delivery of AS or DLA at equivalent molar amounts of AS and AN respectively, *in vivo* tumor growth was significantly inhibited on day 14 in A549 xenografts compared to controls (Fig. 6C). Relative change in tumor volume also showed that AS and DLAE significantly reduced tumor growth (Fig. 6D). In contrast, DLA but not AS significantly inhibited tumor growth on day 14 (Fig. 6E), reducing relative growth by \sim 50% in PC9 xenografts compared to controls (Fig. 6F). Representative gross tumors are shown in Fig. S5. Both DLA and AS were well tolerated and animal weights remained stable during the 14-day treatment (Fig. 6A and 6B).

Discussion

In this study, dried leaves of *A. annua* (DLA) were as effective as AS at inhibiting tumor growth of A549 xenografts. Others showed that AN derivatives successfully inhibited tumor growth in NSCLC xenografts (Efferth, 2017) and growth inhibition of A549-induced tumors by AS in this study was consistent with Ma's xenograft study (Ma et al., 2011). Although A549 cells seemed more responsive to AS than DLAE *in vitro*, growth inhibition of A549 xenografts by DLA was statistically equivalent to that of AS *in vivo*. In PC9 xenografts, however, DLA was more effective than AS in slowing tumor growth. The improved efficacy of AN delivered as DLA *in vivo* compared to its efficacy *in vitro* may be due to increased bioavailability of DLA (Weathers et al., 2011; Weathers et al., 2014), improved AN intestinal permeability (Desrosiers and Weathers, 2017), or potentially by reduced cytochrome P-450 liver metabolism of AN (Wei et al., 2015). Other phytochemicals in DLA that have demonstrated anticancer activity may also directly or indirectly enhance AN's cytotoxicity (Ferreira et al., 2010).

In vitro evidence demonstrated that, comparable to AS, DLAE induced cytotoxicity in NSCLC cells, so DLAE was used to study mechanism of action. AS and DLAE inhibited proliferation of three NSCLC lines in a dose-dependent manner in the micromolar range, but with differences in intensity between cell lines. DLAE vs. AS effects could be

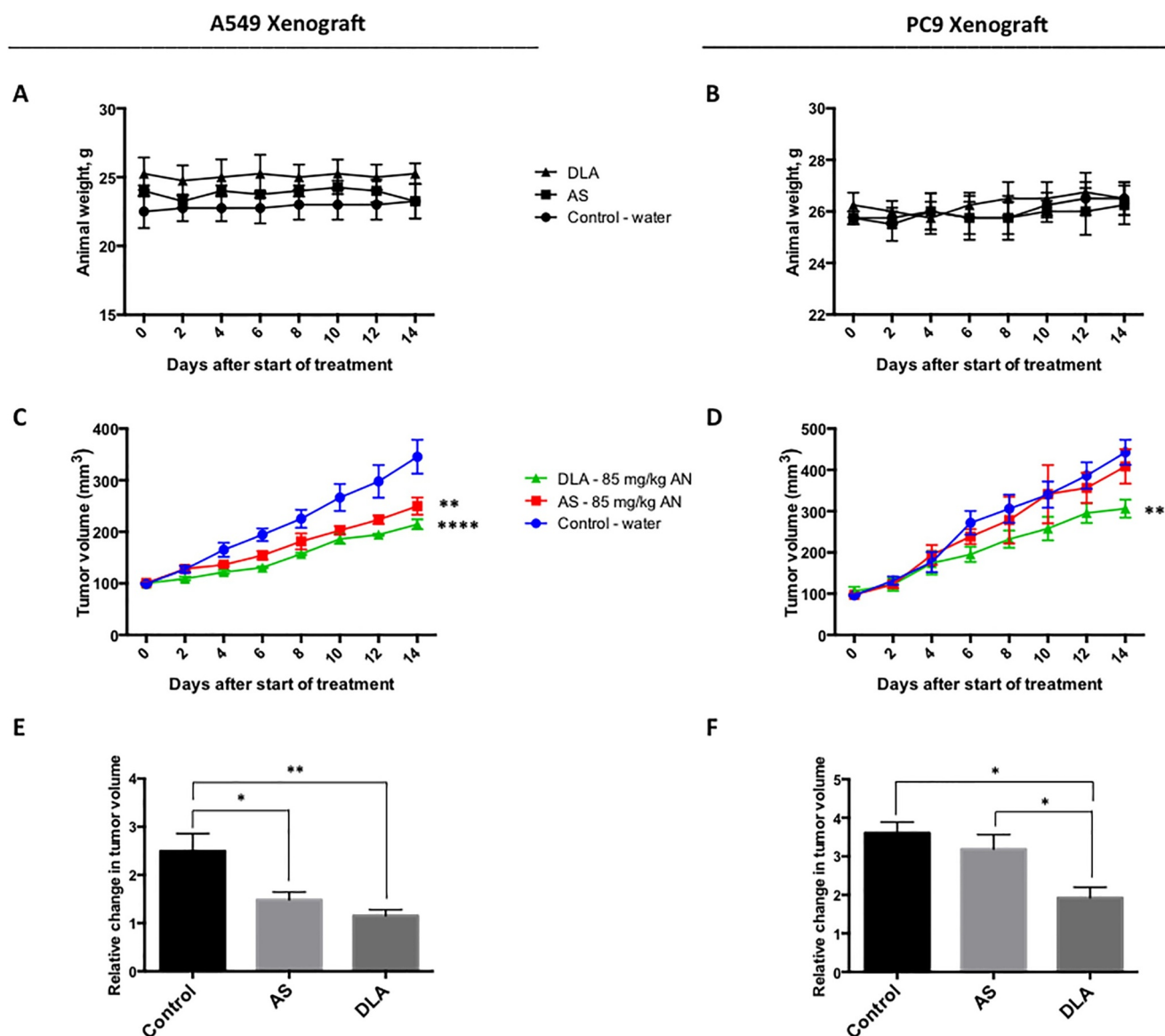


Fig. 6. DLA suppresses tumor growth in A549 and PC9 xenografts. The effect of *p.o.* AS or DLA at equivalent molar dose of 85 mg/kg AN daily for 14 days in A549 or PC9 xenografted mice on (A, B) mean body weight, (C, D) mean tumor volume normalized to average day-0 tumor volume of all animals (** $p < 0.01$, *** $p < 0.001$, compared to controls), or (E, F) mean relative change in tumor volume for each animal (* $p < 0.05$, ** $p < 0.01$) measured from 4 animals per cohort.

explained by differences in driver mutations, differences in amount, location or metabolic rate of iron, or differences in antioxidative profiles, expression of antioxidant enzymes or other adaptive mechanisms to ROS (Lai et al., 2013).

AN derivatives are less cytotoxic to normal cells than cancer cells (Lai et al., 2013), including lung fibroblasts (Mi et al., 2015). In this study HDFs were also less sensitive to AS or DLAE than the neoplastic cells examined. Reduced sensitivity of normal cells, although still debated, may be due to better regulation of intracellular free iron (Lai et al., 2013).

Artemisinins can induce cell cycle arrest in G1 or G2/M phases in NSCLC cells depending on compound and cancer type (Efferth, 2017). In this study, DLAE induced G2/M arrest in both PC9 and H1299 cell lines, but DLAE-treated A549 cells were arrested in G1 phase. AS had the same effects as DLAE except in A549 cells where AS had no effect on cell cycle, contrary to Zhao's study showing AS induced G2/M arrest (Zhao et al., 2011). Others, however, showed that AS induced G1 arrest in both A549 and H1299 cells (Tong et al., 2016). Increased phosphorylated histone H3 protein after 24 h treatment with either AS or DLAE in PC9 and H1299 cells further showed via a mitotic marker

(Gurley et al., 1978) that both drugs impeded mitosis.

There were fewer migratory cells in both PC9 and A549 wound healing assays after 24 h treatment with DLAE compared to controls. Although Tong's study showed AS reduced migration of A549 cells (Tong et al., 2016), there was no difference in our cells after 24 h AS treatment compared to controls. Tong's study used low serum (1%), but not mitomycin C suggesting differences could be due to increased sensitivity to both mitomycin C and low serum. Neither AS nor DLAE showed any effect on H1299 cell migration compared to controls. While AS reportedly reduced H1299 cell migration, results were based on inhibition of matrix metalloproteinase activity and the Wnt/ β -catenin signaling pathway, not a wound healing assay (Tong et al., 2016).

Western blots revealed activation of caspase-3, -8, and -9 in PC9 and A549 cells, but only caspase-3 and -9 in H1299 cells suggesting that AS and DLAE induces apoptosis through the intrinsic mitochondrial apoptotic pathway in all three cell lines and additionally through the extrinsic pathway in two of the cell lines. Although AN derivatives mainly induce apoptosis in cancer cells through the intrinsic pathway (Efferth, 2017), they can stimulate the extrinsic pathway through up-regulation of death receptor DR5 (Das, 2015). Involvement

of both apoptotic pathways is consistent with multiple reports of NSCLC cells treated with AN derivatives as evidenced by activated caspase-3, -8, and -9 (Mi et al., 2015; Gao et al., 2013). ROS was postulated to play a role in caspase-8 mediated apoptosis possibly by AN-induced up-regulation of death receptor transcription, which may act upstream of mitochondrial-activation of caspase-3 (Lu et al., 2010; He et al., 2010). Activating the mitochondrial pathway or co-activating mitochondrial and death receptor pathways of apoptosis are likely determined by the location in the cell where ROS is stimulated by AN interaction with iron (Lai et al., 2013).

Conclusion

To our knowledge this is the first study showing dried leaf *Artemisia annua* (DLA) inhibited tumor growth. Using DLAE to study mechanism, we showed that DLAE is cytotoxic to human NSCLC cells and mechanistically similar to AS by slowing proliferation, stimulating cell cycle arrest and inducing apoptosis. DLAE also inhibited migration of A549 and PC9 NSCLC cells. Moreover, DLA inhibited A549 and PC9 induced tumor growth, whereas AS only inhibited A549 tumor growth. Together these results suggest DLA is a novel therapeutic for possible treatment of NSCLC and potentially other AN-sensitive cancers.

Conflict of interest

We confirm there are no known conflicts of interest associated with this publication and there has been no significant financial support for this study that could have influenced its outcome.

Acknowledgments

Authors thank WPI Professors Amity Manning, Glenn Gaudette, Tanja Dominko, Raymond Page, Dr. Melissa Towler, Ms. Alexis Mittelman for materials, advice and technical assistance, and Prof. J. Plaizier-Vercammen, Farmaceutische Technologie & Fysische Farmacie, Belgium for artesunate. A Kalenian award and WPI each provided partial support.

Supplementary materials

Supplementary material associated with this article can be found, in the online version, at [doi:10.1016/j.phymed.2018.09.167](https://doi.org/10.1016/j.phymed.2018.09.167).

References

Desrosiers, M.R., Weathers, P.J., 2017. Artemisinin permeability via Caco-2 cells increases after simulated digestion of *Artemisia annua* leaves. *J. Ethnopharmacol.* 210, 254–259.

Duke, J.A., 1992. Handbook of Phytochemical Constituent Grass, Herbs and Other Economic Plants. CRC press.

Efferth, T., 2017. From ancient herb to versatile, modern drug: *Artemisia annua* and artemisinin for cancer therapy. *Seminars in Cancer Biology* 46, 65–83.

Efferth, T., Benakis, A., Romero, M.R., Tomicic, M., Rauh, R., Steinbach, D., Häfer, R., Stamminger, T., Oesch, F., Kaina, B., 2004. Enhancement of cytotoxicity of artemisinins toward cancer cells by ferrous iron. *Free Radic. Biol. Med.* 37 (7), 998–1009.

Efferth, T., Herrmann, F., Tahrani, A., Wink, M., 2011. Cytotoxic activity of secondary metabolites derived from *Artemisia annua* L. towards cancer cells in comparison to its designated active constituent artemisinin. *Phytomedicine* 18 (11), 959–969.

Efferth, T., Sauerbrey, A., Olbrich, A., Gebhart, E., Rauch, P., Weber, H.O., Hengstler,

J.G., Halatsch, M.-E., Volm, M., Tew, K.D., 2003. Molecular modes of action of artesunate in tumor cell lines. *Mol. Pharmacol.* 64 (2), 382–394.

Elfawal, M.A., Towler, M.J., Reich, N.G., Golenbock, D., Weathers, P.J., Rich, S.M., 2012. Dried whole plant *Artemisia annua* as an antimalarial therapy. *PLoS One* 7 (12), e52746.

Ferreira, J.F., Luthria, D.L., Sasaki, T., Heyerick, A., 2010. Flavonoids from *Artemisia annua* L. as antioxidants and their potential synergism with artemisinin against malaria and cancer. *Molecules* 15 (5), 3135–3170.

Gao, W., Xiao, F., Wang, X., Chen, T., 2013. Artemisinin induces A549 cell apoptosis dominantly via a reactive oxygen species-mediated amplification activation loop among caspase-9,-8 and-3. *Apoptosis* 18 (10), 1201–1213.

Gurley, L.R., D'anna, J.A., Barham, S.S., Deaven, L.L., Tobey, R.A., 1978. Histone phosphorylation and chromatin structure during mitosis in Chinese hamster cells. *FEBS J.* 84 (1), 1–15.

He, Q., Shi, J., Shen, X.-L., An, J., Sun, H., Wang, L., Hu, Y.-J., Sun, Q., Fu, L.-C., Sheikh, M.S., 2010. Dihydroartemisinin upregulates death receptor 5 expression and cooperates with TRAIL to induce apoptosis in human prostate cancer cells. *Cancer Biol. Therap.* 9 (10), 819–824.

Hooda, J., Cadinu, D., Alam, M.M., Shah, A., Cao, T.M., Sullivan, L.A., Brekken, R., Zhang, L., 2013. Enhanced heme function and mitochondrial respiration promote the progression of lung cancer cells. *PLoS One* 8 (5), e63402.

Kwok, J.C., Richardson, D.R., 2002. The iron metabolism of neoplastic cells: alterations that facilitate proliferation? *Crit. Rev. Oncol. Hematol.* 42 (1), 65–78.

Lai, H., Singh, N.P., 1995. Selective cancer cell cytotoxicity from exposure to dihydroartemisinin and holotransferrin. *Cancer Lett.* 91 (1), 41–46.

Lai, H.C., Singh, N.P., Sasaki, T., 2013. Development of artemisinin compounds for cancer treatment. *Invest. New Drugs* 31 (1), 230–246.

Lee, I.-S., Hufford, C.D., 1990. Metabolism of antimalarial sesquiterpene lactones. *Pharmacol. Therapeut.* 48 (3), 345–355.

Lu, Y.-Y., Chen, T.-S., Wang, X.-P., Li, L., 2010. Single-cell analysis of dihydroartemisinin-induced apoptosis through reactive oxygen species-mediated caspase-8 activation and mitochondrial pathway in ASTC-a-1 cells using fluorescence imaging techniques. *J. Biomed. Opt.* 15 (4), 046028–046028-16.

Ma, H., Yao, Q., Zhang, A.-M., Lin, S., Wang, X.-X., Wu, L., Sun, J.-G., Chen, Z.-T., 2011. The effects of artesunate on the expression of EGFR and ABCG2 in A549 human lung cancer cells and a xenograft model. *Molecules* 16 (12), 10556–10569.

Mi, Y.-j., Geng, G.-j., Zou, Z.-z., Gao, J., Luo, X.-y., Liu, Y., Li, N., Li, C.-l., Chen, Y.-q., Yu, X.-y., 2015. Dihydroartemisinin inhibits glucose uptake and cooperates with glycolysis inhibitor to induce apoptosis in non-small cell lung carcinoma cells. *PLoS One* 10 (3), e0120426.

O'Neill, P.M., Posner, G.H., 2004. A medicinal chemistry perspective on artemisinin and related endoperoxides. *J. Med. Chem.* 47 (12), 2945–2964.

Saito, S., Espinoza-Mercado, F., Liu, H., Sata, N., Cui, X., Soukiasian, H.J., 2017. Current status of research and treatment for non-small cell lung cancer in never-smoking females. *Cancer Biol. Therap.* 18 (6), 359–368.

Tong, Y., Liu, Y., Zheng, H., Zheng, L., Liu, W., Wu, J., Ou, R., Zhang, G., Li, F., Hu, M., 2016. Artemisinin and its derivatives can significantly inhibit lung tumorigenesis and tumor metastasis through Wnt/ β -catenin signaling. *Oncotarget* 7 (21), 31413.

Wang, J., Zhang, C.-J., Chia, W.N., Loh, C.C., Li, Z., Lee, Y.M., He, Y., Yuan, L.-X., Lim, T.K., Liu, M., 2015. Haem-activated promiscuous targeting of artemisinin in *Plasmodium falciparum*. *Nature Commun.* (6), 10111.

Weathers, P.J., Arsenaault, P.R., Covello, P.S., McMickle, A., Teoh, K.H., Reed, D.W., 2011. Artemisinin production in *Artemisia annua*: studies in planta and results of a novel delivery method for treating malaria and other neglected diseases. *Phytochem. Rev.* 10 (2), 173–183.

Weathers, P.J., Elfawal, M.A., Towler, M.J., Acquah-Mensah, G.K., Rich, S.M., 2014. Pharmacokinetics of artemisinin delivered by oral consumption of *Artemisia annua* dried leaves in healthy vs. *Plasmodium chabaudi*-infected mice. *J. Ethnopharmacol.* 153 (3), 732–736.

Weathers, P.J., Towler, M.J., 2014. Changes in key constituents of clonally propagated *Artemisia annua* L. during preparation of compressed leaf tablets for possible therapeutic use. *Ind. Crops Prod.* (62), 173–178.

Wei, S., Ji, H., Yang, B., Ma, L., Bei, Z., Li, X., Dang, H., Yang, X., Liu, C., Wu, X., Chen, J., 2015. Impact of chrysofenetin on the pharmacokinetics and anti-malarial efficacy of artemisinin against *Plasmodium berghei* as well as *in vitro* CYP450 enzymatic activities in rat liver microsomes. *Malar. J.* 14 (1), 432.

WHO, 2015. Guidelines for the Treatment of Malaria, Third Edition. World Health Organization.

Zhao, Y., Jiang, W., Li, B., Yao, Q., Dong, J., Cen, Y., Pan, X., Li, J., Zheng, J., Pang, X., 2011. Artesunate enhances radiosensitivity of human non-small cell lung cancer A549 cells via increasing no production to induce cell cycle arrest at G2/M phase. *Int. Immunopharmacol.* 11 (12), 2039–2046.